

ACSL1, CH25H, GPCPD1, and PLA2G12A as the potential lipid-related diagnostic biomarkers of acute myocardial infarction

Zheng-Yu Liu^{1,2,3,*}, Fen Liu^{2,3,4,*}, Yan Cao^{2,3,5}, Shao-Liang Peng^{2,6}, Hong-Wei Pan^{1,2,3}, Xiu-Qin Hong^{2,3,4}, Peng-Fei Zheng^{1,2,3}

¹Department of Cardiology, Hunan Provincial People's Hospital, Changsha 410000, China

²Department of Epidemiology, Hunan Provincial People's Hospital (The First Affiliated Hospital of Hunan Normal University), Changsha 410000, China

³Clinical Medicine Research Center of Heart Failure of Hunan Province, Changsha 410000, China

⁴The First Affiliated Hospital of Hunan Normal University (Hunan Provincial People's Hospital), Changsha 410000, China

⁵Department of Emergency, Hunan Provincial People's Hospital, Changsha 410000, China

⁶Clinical Data Center, Hunan Provincial People's Hospital, Changsha 410000, China

*Equal contribution and co-first authors

Correspondence to: Peng-Fei Zheng, Xiu-Qin Hong; **email:** peifengzheng@hunnu.edu.cn, xiuqinhong0528@hunnu.edu.cn

Keywords: lipid, acute myocardial infarction, bioinformatics analysis, machine learning, gene

Received: October 24, 2022

Accepted: February 13, 2023

Published: February 24, 2022

Copyright: © 2023 Liu et al. This is an open access article distributed under the terms of the [Creative Commons Attribution License](https://creativecommons.org/licenses/by/3.0/) (CC BY 3.0), which permits unrestricted use, distribution, and reproduction in any medium, provided the original author and source are credited.

ABSTRACT

Lipid metabolism plays an essential role in the genesis and progress of acute myocardial infarction (AMI). Herein, we identified and verified latent lipid-related genes involved in AMI by bioinformatic analysis. Lipid-related differentially expressed genes (DEGs) involved in AMI were identified using the GSE66360 dataset from the Gene Expression Omnibus (GEO) database and R software packages. Gene ontology (GO) and Kyoto Encyclopedia of Genes and Genomes (KEGG) pathway enrichment analyses were conducted to analyze lipid-related DEGs. Lipid-related genes were identified by two machine learning techniques: least absolute shrinkage and selection operator (LASSO) regression and support vector machine recursive feature elimination (SVM-RFE). The receiver operating characteristic (ROC) curves were used to describe diagnostic accuracy. Furthermore, blood samples were collected from AMI patients and healthy individuals, and real-time quantitative polymerase chain reaction (RT-qPCR) was used to determine the RNA levels of four lipid-related DEGs. Fifty lipid-related DEGs were identified, 28 upregulated and 22 downregulated. Several enrichment terms related to lipid metabolism were found by GO and KEGG enrichment analyses. After LASSO and SVM-RFE screening, four genes (*ACSL1*, *CH25H*, *GPCPD1*, and *PLA2G12A*) were identified as potential diagnostic biomarkers for AMI. Moreover, the RT-qPCR analysis indicated that the expression levels of four DEGs in AMI patients and healthy individuals were consistent with bioinformatics analysis results. The validation of clinical samples suggested that 4 lipid-related DEGs are expected to be diagnostic markers for AMI and provide new targets for lipid therapy of AMI.

INTRODUCTION

Acute myocardial infarction (AMI) has become the main cause of hospitalization and death worldwide,

seriously threatening human health. Previous studies have suggested that AMI is a complex syndrome with multifactorial disorders. Its risk factors include early family history, smoking, hypertension, dyslipidemia,

and diabetes [1–4]. The rupture of vulnerable and lipid-overloaded coronary atherosclerotic plaques can induce the formation of acute thrombus, leading to acute occlusion of blood vessels and progressing to AMI [5]. Dyslipidemia, especially elevated levels of low-density lipoprotein (LDL) cholesterol, is believed to play a key role in the pathogenesis of atherosclerosis [6, 7]. Atherogenesis begins when residues of LDL cholesterol, chylomicron, and very low-density lipoprotein (VLDL) cholesterol molecules enter the artery intima. Then, lipid radicals are oxidized and endocytosed by macrophages, followed by the formation of foam cells [6]. Previous studies have demonstrated that every 1% reduction in LDL cholesterol levels is associated with a 1% reduction in AMI risk [8, 9]. Currently, statin therapy has become the cornerstone for cholesterol-lowering drug therapy for coronary heart disease and AMI patients. Moreover, the combination of PCSK9 inhibitors with statins is recommended to reduce the risk of major adverse cardiovascular events (MACEs) in AMI patients [10]. However, the combination of lipid-lowering therapy still cannot eliminate the risk of MACEs in AMI patients. This might be partly because some lipid-related genes have not been identified. Therefore, identifying new lipid metabolism-related genes associated with AMI will help develop new lipid-lowering drugs to reduce the risk of MACEs in AMI patients.

Microarray analysis is an innovative and practical method to discern susceptibility genes to deal with coronary heart disease [11] and AMI [12]. Nevertheless, microarray analysis using differentially expressed genes (DEGs) might have limitations in reproducibility and sensitivity [13, 14]. Machine learning can enhance the prediction and accuracy of these key genes discerned using traditional microarrays or next-generation sequencing data [15]. The most frequently used machine learning techniques include the least absolute shrinkage and selection operator (LASSO) regression and support vector machine recursive feature elimination (SVM-RFE) algorithm [16]. Meanwhile, the combined application of LASSO regression and SVM-RFE algorithm in identifying new lipid-related genes involved in AMI has not been conducted. Therefore, in the present study, we analyzed the GSE66360 dataset from different perspectives: 1) DEGs among lipid-related AMI genes were identified using the “limma” R package and GO and KEGG pathway enrichment analyses. 2) Machine learning methods were applied to large-scale screening and diagnostic identification of AMI-related molecular markers. 3) Lipid-related gene expression levels screened by machine learning were validated using clinical cases.

RESULTS

Identification of lipid-related DEGs in GSE66360

Due to the limitations of chip detection technology, a total of 673 lipid-related genes in 49 AMI samples and 50 normal samples were used to analyze DEGs. After data normalization and removal of batch differences, 50 lipid-related genes were identified, 28 upregulated and 22 downregulated (Table 1). These 50 lipid-related DEGs can be visualized in the volcano plot and heatmap (Figure 1A, 1B). The expression pattern between the two groups was highlighted based on the box plot (Figure 2). Among them, the top three upregulated genes were *ACSSLI* (Acyl-CoA Synthetase Long-Chain Family Member 1), *PLBD1* (Phospholipase B Domain Containing 1), and *CH25H* (Cholesterol 25-Hydroxylase). Meanwhile, the top three down-regulated genes were *ELOVL4* (*ELOVL* Fatty Acid Elongase 4), *TNFAIP8L2* (*TNF* Alpha Induced Protein 8 Like 2), and *CYP2E1* (Cytochrome P450 Family 2 Subfamily E Member 1).

Correlation analysis of lipid-related DEGs

The 50 lipid-related DEGs in the GSE66360 were significantly correlated by the Pearson correlation analysis (Figure 3). The positive correlation between the *PLBD1* and *ACSLI* was strongest; and the *CYP4F2* had the most obvious negative correlation with *PTPN13*. Moreover, the *ACSLI* was positively related to *GPCPD1* and *CH25H*; the *CH25H* was positively related to *GPCPD1* and *ACSLI*; the *PLA2G12A* was positively related to *GPCPD1* while negatively related to *CH25H*.

Functional analyses of lipid-related DEGs

The biological functions of lipid-related DEGs were determined by GO and KEGG enrichment analyses using R software. The most enriched GO terms were fatty acid metabolic, glycerolipid metabolic, and phospholipid metabolic processes (biological processes, Figure 4A); intrinsic component of endoplasmic reticulum membrane, integral component of endoplasmic reticulum membrane, and lipid droplet (cellular components, Figure 4B); oxidoreductase activity, iron ion binding, and acyltransferase activity (molecular functions, Figure 4C). The KEGG enrichment analyses showed that lipid-related DEGs were involved in the arachidonic acid metabolism, glycerophospholipid metabolism, chemical carcinogenesis-DNA adducts, and the PPAR signaling pathway (Figure 5). The details of these analyses can also be found in Supplementary Table 1.

Table 1. The 50 differentially expressed lipid-related genes in AMI samples compared to healthy samples.

Gene symbol	Log₂FC	Changes	p-value	Adjusted p-value
ACSL1	2.1443758	Up	9.76E-14	6.57E-11
PLBD1	2.0855158	Up	1.33E-08	1.49E-06
CH25H	1.561894	Up	1.67E-10	5.63E-08
PTGS2	1.4727308	Up	1.64E-04	2.56E-03
CYP4F3	1.4307856	Up	2.77E-07	1.35E-05
CD36	1.3377248	Up	1.25E-08	1.49E-06
G0S2	1.3051173	Up	7.36E-06	2.06E-04
LPCAT2	1.274232	Up	1.13E-07	6.95E-06
CYP1B1	1.081695	Up	2.57E-07	1.35E-05
MBOAT2	0.996586	Up	9.09E-08	6.80E-06
DGAT2	0.9506635	Up	4.65E-07	2.09E-05
GPCPD1	0.9145163	Up	2.38E-05	5.52E-04
ABCA1	0.8308084	Up	3.50E-08	2.94E-06
BMX	0.8267136	Up	9.28E-07	3.90E-05
PTGS1	0.8263128	Up	8.69E-05	1.46E-03
MBOAT7	0.8240098	Up	3.66E-06	1.29E-04
SGMS2	0.8165743	Up	5.71E-04	6.86E-03
ABHD5	0.7901841	Up	1.44E-09	3.23E-07
GK3P	0.7584331	Up	1.02E-04	1.68E-03
ALOX12	0.7568656	Up	4.36E-03	3.45E-02
TNFRSF21	0.7529465	Up	2.53E-03	2.27E-02
TBXAS1	0.7461727	Up	3.82E-05	7.34E-04
CYP27A1	0.6990032	Up	2.48E-06	9.27E-05
STARD4	0.6983926	Up	3.56E-03	2.89E-02
ASAH1	0.6750605	Up	4.30E-05	7.82E-04
CYP4F2	0.6721891	Up	4.74E-06	1.59E-04
GK	0.6464259	Up	2.46E-04	3.52E-03
ALOX5AP	0.6346144	Up	1.04E-03	1.13E-02
SLC44A3	-0.590564	Down	1.18E-03	1.20E-02
CEPT1	-0.599105	Down	1.17E-03	1.20E-02
MCEE	-0.609681	Down	2.24E-03	2.12E-02
PLA2G12A	-0.612271	Down	6.79E-06	1.99E-04
PNPLA4	-0.612941	Down	2.48E-03	2.27E-02
NFYB	-0.623073	Down	2.92E-04	4.09E-03
CROT	-0.628778	Down	2.87E-05	6.43E-04
GGPS1	-0.647568	Down	3.19E-05	6.58E-04
ARV1	-0.654258	Down	3.44E-05	6.81E-04
INSIG2	-0.663348	Down	6.01E-03	4.40E-02
THEM4	-0.748033	Down	2.99E-05	6.49E-04
PHYH	-0.755787	Down	2.36E-03	2.21E-02

PIK3C2B	-0.764005	Down	4.21E-04	5.45E-03
PTPN13	-0.771322	Down	3.25E-04	4.47E-03
AGPAT5	-0.799176	Down	8.56E-05	1.46E-03
ORMDL2	-0.803203	Down	1.43E-03	1.44E-02
GDPD3	-0.810763	Down	4.53E-04	5.75E-03
LCLAT1	-0.828645	Down	7.23E-04	8.25E-03
HSD11B1	-0.973808	Down	1.14E-07	6.95E-06
CYP2E1	-1.067542	Down	5.45E-06	1.75E-04
TNFAIP8L2	-1.222639	Down	8.47E-06	2.19E-04
ELOVL4	-1.35438	Down	2.82E-07	1.35E-05

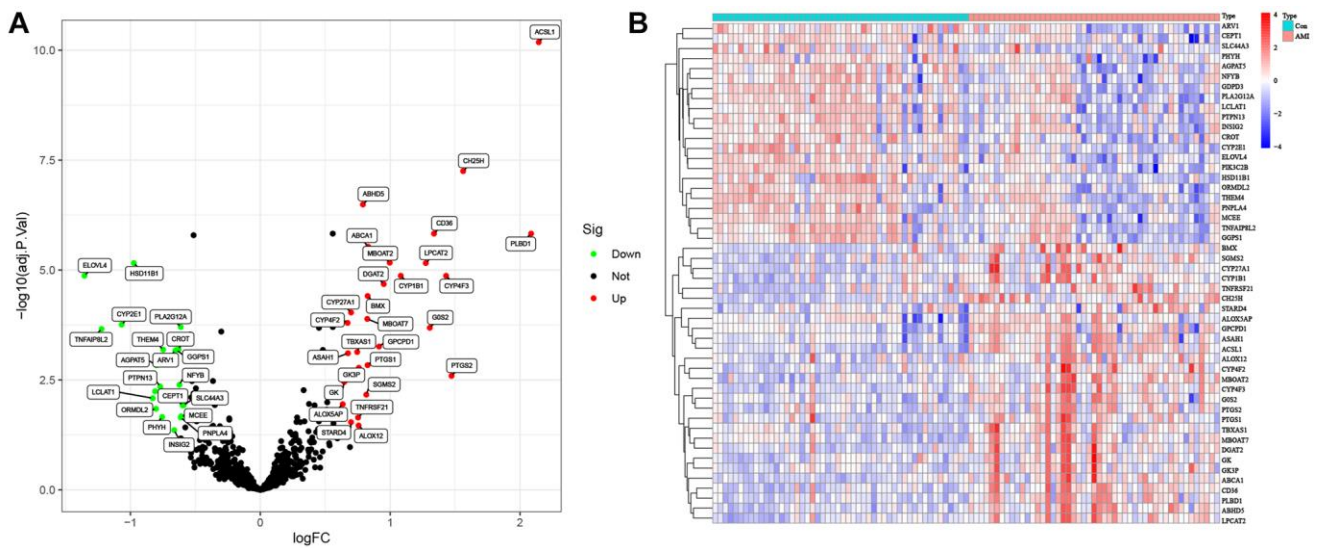


Figure 1. Lipid-related differentially expressed genes (DEGs) in AMI and healthy samples. (A) Volcano plot of the 673 lipid-related DEGs. Red dots represent significantly upregulated genes, and green significantly downregulated genes. (B) Heatmap of the 50 lipid-related DEGs in AMI and healthy samples.

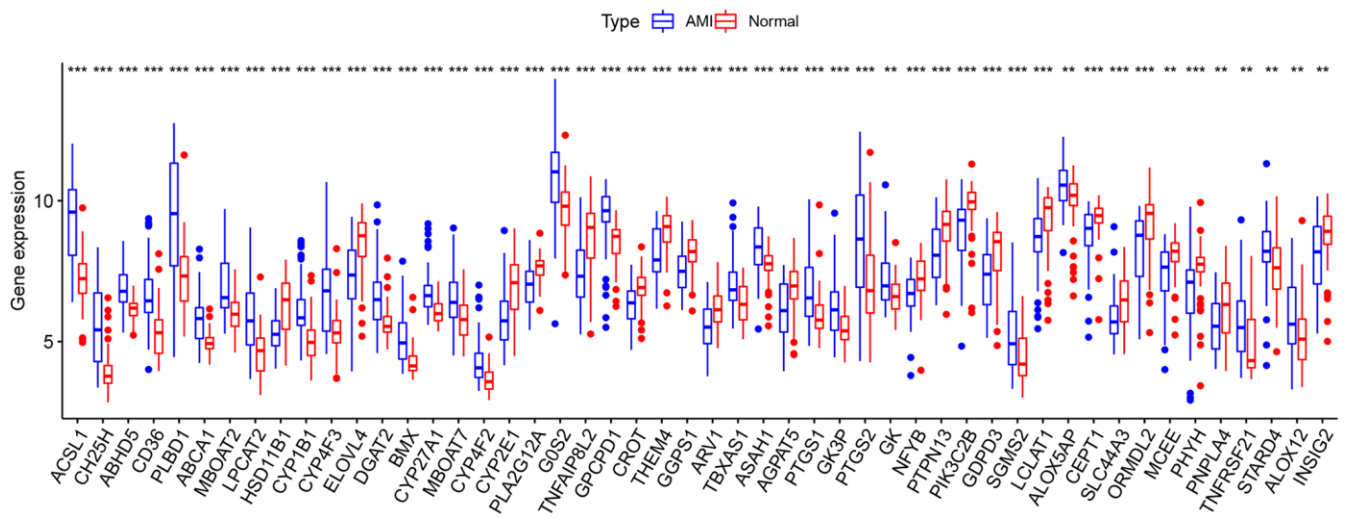


Figure 2. Box plot of 50 lipid-related differentially expressed genes (DEGs) in AMI and healthy samples. * $p < 0.05$; ** $p < 0.01$; *** $p < 0.005$.

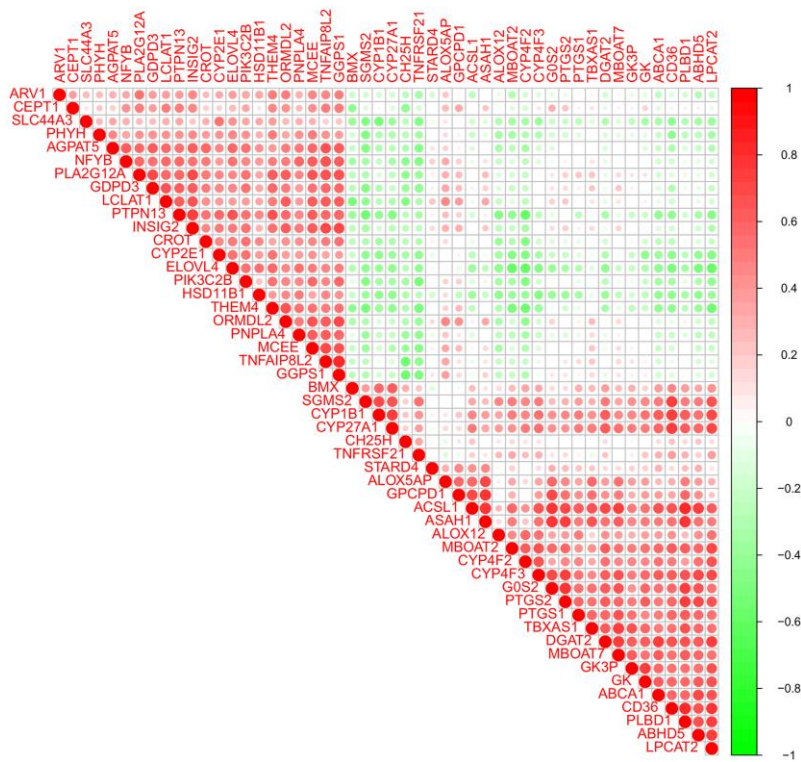


Figure 3. Pearson correlation analysis of the 50 lipid-related differentially expressed genes (DEGs).

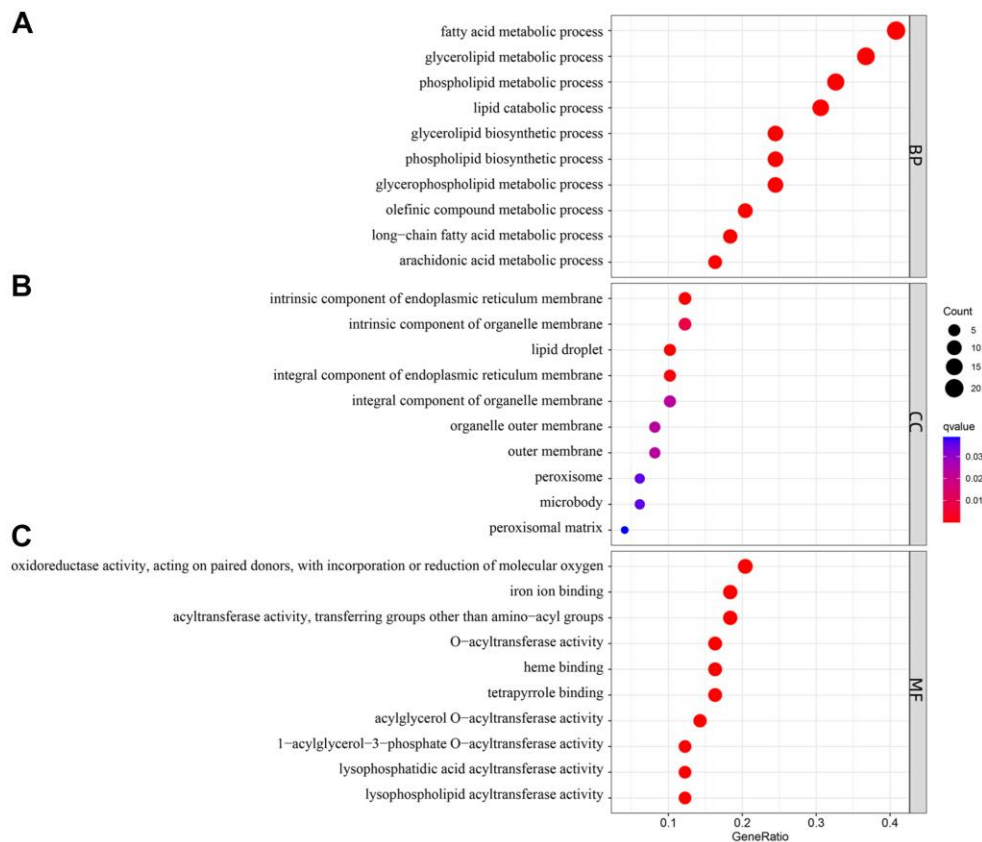


Figure 4. Gene Ontology (GO) enrichment analysis of 50 differentially expressed genes (DEGs). Abbreviations: (A) BP: biological process; (B) CC: cellular component; (C) MF: molecular function.

Screening key DEGs by LASSO logistic regression and SVM-RFE

The LASSO logistic regression identified 15 lipid-related genes based on the optimum λ value (Figure 6A), whereas the SVM-RFE algorithm identified four genes (Figure 6B). Four overlap genes including *ACSL1*, *CH25H*, *GPCPD1* (Glycerophosphocholine Phosphodiesterase 1), and *PLA2G12A* (Phospholipase A2 Group XIIA) were identified by LASSO and SVM-RFE algorithm as key lipid-related DEGs for subsequent analysis (Figure 6C). In addition, other 14 genes identified by LASSO regression are listed in Supplementary Table 2.

ROC curves between AMI and control groups

The expression of the four lipid-related DEGs between the AMI and control samples of the GSE66360 dataset were analyzed using R software, and the ROC curves were constructed. The area under the curve (AUC), unified with specificity and sensitivity, verified the intrinsic validity of diagnostic tests [17]. Four lipid-related DEGs had a superior diagnostic value for AMI. Among them, the gene with the most significant diagnostic value was *ACSL1* (AUC = 0.878). The other genes are: *CH25H* (AUC = 0.853), *GPCPD1* (AUC = 0.819), and *PLA2G12A* (AUC = 0.747) (Figure 7). These four lipid-related DEGs can be considered underlying diagnostic biomarkers for AMI.

Validation by RT-qPCR

To verify the dependability of the GSE66360 dataset, RT-qPCR was used to validate the expression levels of the above four lipid-related genes in clinical samples. The clinical data of AMI and control groups are summarized in Table 2. The RT-qPCR results suggested in Figure 8, that the expression level of *PLA2G12A* ($p = 2.8e-08$) increased in controls compared to the AMI group, while *ACSL1* ($p = 2.4e-09$), *CH25H* ($p = 0.023$), and *GPCPD1* ($p = 1.3e-08$) were higher in AMI group. Hence, the RT-qPCR results performed were consistent with the main bioinformatic analysis.

Verification of the potential biomarkers for AMI

Furthermore, we analyzed the gene expression levels in the AMI group and healthy individuals using the ROC curve to verify the diagnostic value of the four screened lipid-related genes as shown in Figure 9. The AUC values of *ACSL1*, *CH25H*, *GPCPD1* and *PLA2G12A* were 0.846 [95% confidence interval (CI): 0.764–0.929], 0.632 (95% CI: 0.517–0.747), 0.830 (95% CI: 0.749–0.912), and 0.822 (95% CI: 0.744–0.901), respectively. This result showed that these lipid-related DEGs are diagnostic biomarkers for AMI.

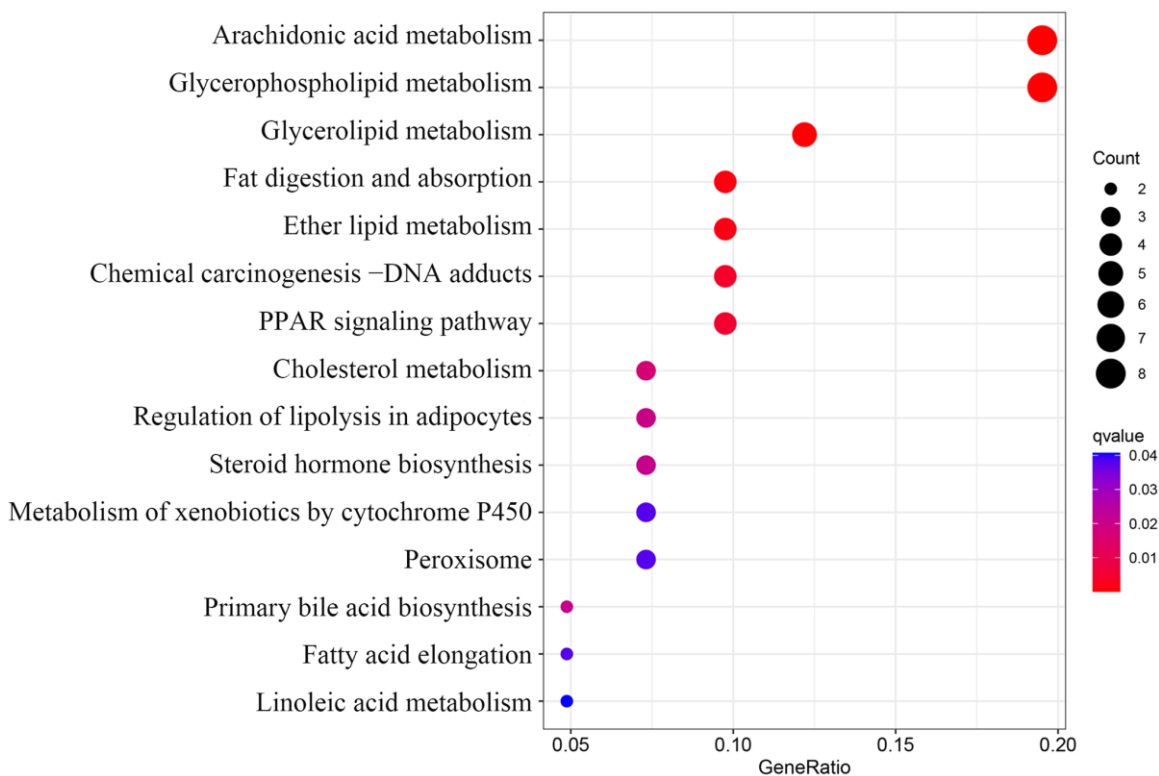


Figure 5. Kyoto Encyclopedia of Genes and Genomes (KEGG) pathway analysis of 50 lipid-related differentially expressed genes (DEGs).

DISCUSSION

Acute myocardial infarction (AMI) refers to hypoxia caused by coronary atherosclerosis stenosis and myocardial necrosis caused by acute and persistent ischemia [18]. Dyslipidemia is a known risk factor for AMI [19], and lipid-lowering therapy is the treatment cornerstone. Several convincing studies have shown that the combined effect of lowering triglyceride, LDL cholesterol, and total cholesterol levels yield higher cardiovascular risk than lowering LDL cholesterol levels alone [20–22]. The accumulated molecular genetic data indicate that many genes are related to AMI occurrence, including lipid-related genes [23]. However, the lipid-related genes involved in AMI have not been completely identified. Thus, it is necessary to comprehend the role of lipid-related genes in AMI diagnosis and treatment.

Herein, we retrieved data of AMI patients (GSE66360) and subjected it to differential genes analysis, and identified lipid-related DEGs associated with AMI. Lipid-related DEGs were then subjected to GO and KEGG enrichment analyses. LASSO regression is a machine learning method that recognizes variables by looking for a λ value for a minimal classification error

[24]. SVM-RFE is another machine learning method that finds optimal variables through subtracting SVM-generated feature vectors [25]. We used these two algorithms to screen characteristic variables and created an optimal classification model. Four lipid-related genes (*ACSL1*, *CH25H*, *GPCPD1*, and *PLA2G12A*) were identified based on these two methods, which significantly impact AMI diagnosis. Moreover, the findings of *CH25H* were controversial compared with previous studies and should be interpreted with caution. Nevertheless, the p values of these four lipid-related genes were < 0.05 , verified by RT-qPCR and consistent with our bioinformatic analysis results.

ACSL1 is a key rate-limiting enzyme in lipid metabolism [26], catalyzing the energy production of fatty acids or the production of phospholipids, cholesterol esters, and triglycerides [27]. Previous studies have shown that heart-specific overexpression of *ACSL1* in mice increases triglyceride accumulation in cardiomyocytes [28]. Li et al. demonstrated that inhibiting *ACSL1* expression in the heart can reduce lipid metabolism and promote the regeneration of cardiomyocytes [29]. A cohort study has shown that the expression level of *ACSL1* in peripheral blood leukocytes of AMI patients was higher than that of

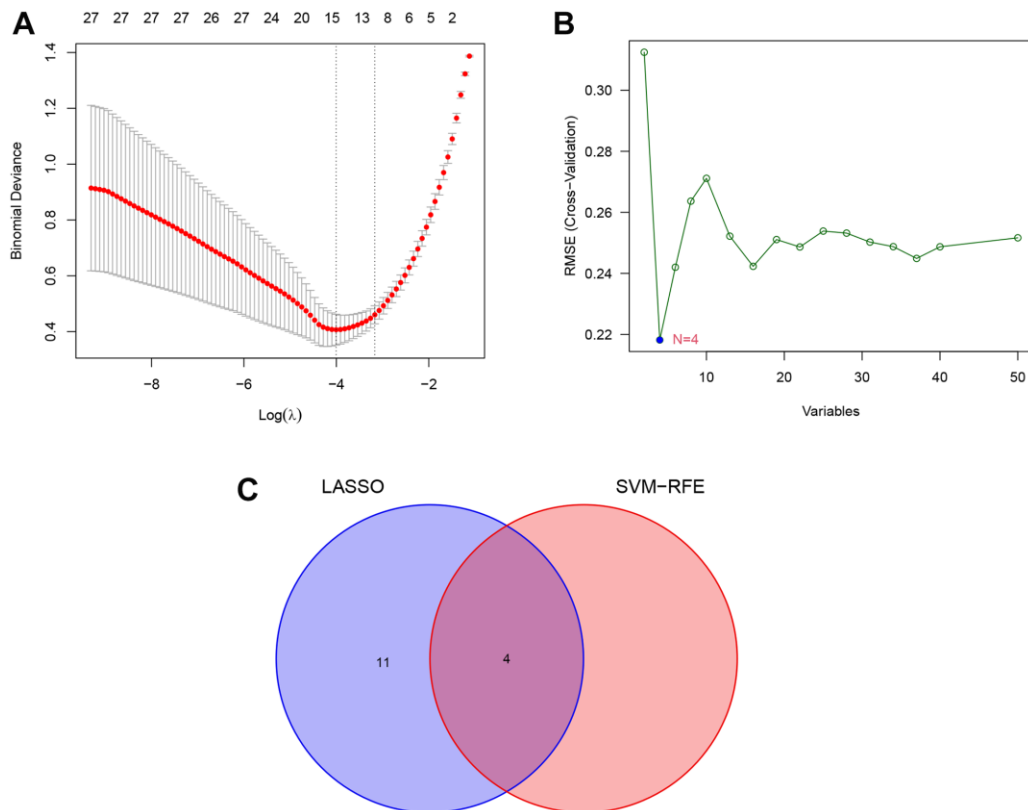


Figure 6. Identification of key lipid-related DEGs by machine learning methods. (A) Least absolute shrinkage and selection operator (LASSO) logistic regression screening of key lipid-related DEGs. (B) Support vector machine-recursive feature elimination (SVM-RFE) algorithm screening of key lipid-related DEGs. (C) Venn diagram of the intersection of diagnostic markers obtained by the two algorithms.

healthy controls, and this high expression was a risk factor for AMI [30]. A recent study confirmed that the overexpression of *ACSL1* can reduce fatty acid β -oxidation and increase plasma triglyceride levels by regulating the *PPAR γ* pathway, which is one of the mechanisms that can promote the pathogenesis of AMI [31]. These results supported the findings of our bioinformatic analysis and suggested that *ACSL1* plays a pathological role in AMI through lipid metabolism and might be a promising AMI biomarker. Moreover, *PLA2G12A* is a secreted phospholipase A2, but its physiological function is largely unclear. In humans, there is a suggestive association between a *PLA2G12A* polymorphism and response to anti-vascular endothelial growth factor therapy in patients with exudative age-related macular degeneration [32]. Alexandros et al. showed that *PLA2G12A* is highly expressed in aortic endothelial cells *in vivo* and may inhibit atherosclerosis by reducing the adhesion properties of vascular endothelial cells, which confirmed *PLA2G12A* as a candidate gene for atherosclerosis protection [33]. This was consistent with our findings that *PLA2G12A* was downregulated in AMI samples and was a protective

gene, possibly by reducing vascular adhesion to decrease AMI incidence.

CH25H regulates cholesterol and lipid metabolism by converting cholesterol to 25-HC, and plays an important role in regulating cellular inflammatory states and cholesterol biosynthesis in endothelial cells and monocytes [34]. *CH25H* and 25-HC were traditionally regarded as key regulators to maintain cholesterol homeostasis by inhibiting sterol regulator-binding protein (SREBP) and liver X receptor (LXR) [35]. Elizabeth et al. showed that 25-HC production promotes the formation of macrophage foam cells and increases susceptibility to atherosclerosis, thereby increasing AMI risk [36]. However, the pro-inflammatory role of *CH25H* in atherosclerosis remains controversial. Other studies have shown that *CH25H* is involved in macrophages' functional endothelium and anti-inflammatory phenotype and that *CH25H* ablation increases susceptibility to atherosclerosis [37]. Our current study suggested that *CH25H* was upregulated in AMI samples, consistent with the Elizabeth et al. results. This contradiction might be partly due to different

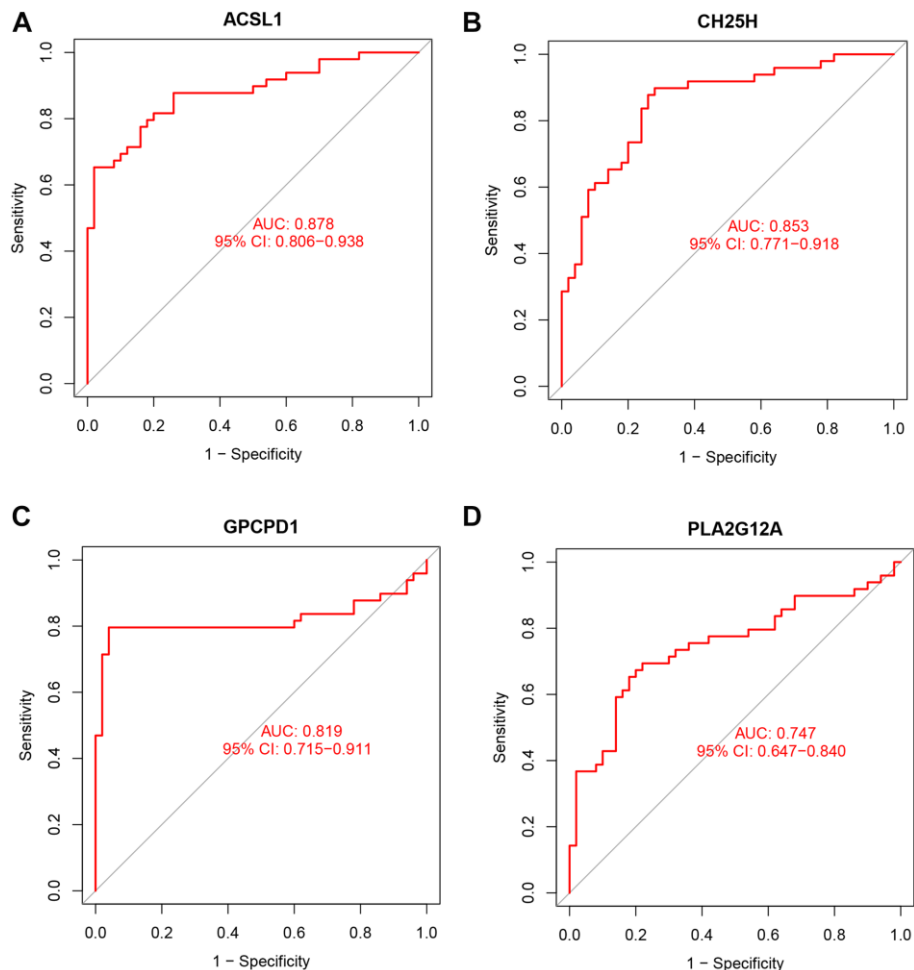


Figure 7. ROC curve analysis. ROC curve of *ACSL1* (A), *CH25H* (B), *GPCPD1* (C), *PLA2G12A* (D) in GSE66360 dataset.

Table 2. Clinical characteristic between control and AMI group.

Characteristic	Control (n = 50)	AMI (n = 50)	p
Male [n (%)] ^a	35 (70.0)	34 (68.0)	0.829
Age (years) ^a	55.16 ± 7.22	56.52 ± 6.79	0.673
BMI (kg/m ²) ^a	20.98 ± 2.74	23.69 ± 3.20	0.305
Smoking [n (%)] ^b	11 (22.0)	23 (46.0)	0.011
Alcohol [n (%)] ^b	13 (26.0)	21 (42.0)	0.091
Hypertension [n (%)] ^b	15 (30.0)	30 (60.0)	0.003
Type 2 Diabetes [n (%)] ^b	10 (20.0)	19 (38.0)	0.047
CK (U/L) ^a	125.84 ± 9.35	1162.1 ± 576.30	6.20E-9
CK-MB (U/L) ^a	15.5 ± 3.06	130.35 ± 19.76	1.14E-11
ApoA1 (g/L) ^a	1.38 ± 0.30	0.96 ± 0.19	0.045
ApoB (g/L) ^a	0.82 ± 0.19	1.01 ± 0.29	0.037
TC (mmol/L) ^a	3.96 ± 0.80	4.12 ± 1.14	0.029
TG (mmol/L) ^a	1.29 ± 0.41	1.50 ± 0.66	0.023
HDL-C (mmol/L) ^a	1.63 ± 0.47	1.10 ± 0.29	0.030
LDL-C (mmol/L) ^a	2.25 ± 0.94	3.57 ± 1.26	0.003
Creatinine (μmol/L) ^a	86.14 ± 13.07	88.98 ± 17.49	0.039
Troponin T (μg/L) ^a	0.04 ± 0.03	3.22 ± 1.19	2.87E-5

Abbreviations: BMI: Body mass index; HDL-C: high-density lipoprotein cholesterol; LDL-C: low-density lipoprotein cholesterol; Apo: Apolipoprotein; TC: Total cholesterol; TG: Triglyceride; CK: creatine kinase; CK-MB: creatine kinase-myocardial band. ^aMean ± SD determined by *t*-test. ^bThe rate or constituent ratio between the different groups was analyzed by the χ^2 test.

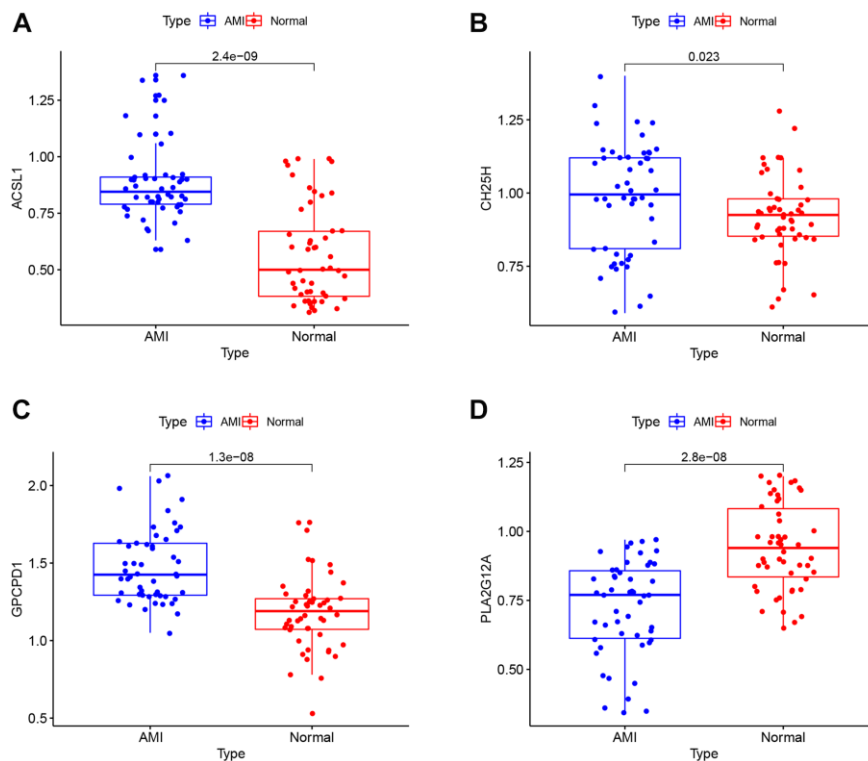


Figure 8. RT-qPCR analysis. The mRNA expression levels of *ACSL1* (A), *CH25H* (B), *GPCPD1* (C), *PLA2G12A* (D) in clinical samples.

experimental conditions requiring further study. Additionally, GPCPD1 is a key enzyme in choline and phospholipid metabolism. GPCPD1 has also been reported to be involved in the complex network of enzymatic reactions regulating choline metabolism [38]. It can cleave glycerophosphocholine to form glycerol-3-phosphate and choline [39]. GPCPD1 has been reported to promote cell migration, metastasis, adhesion, and diffusion in breast, endometrial, and ovarian cancers. However, its biological role in cardiovascular disease remains unclear. Hence, more studies are needed to further verify our current findings.

In the current research, several correlations between four key lipid-related DEGs were also noticed. Correlation analysis indicated that the *ACSL1*, *CH25H*, *GPCPD1*, and *PLA2G12A* genes may influence the occurrence of AMI by synergistically regulating the same lipid metabolic pathway. Meanwhile, the functional analyses were also performed to evaluate the potential biological functions of lipid-related DEGs. The GO enrichment analysis showed that these genes were closely related to fatty acid metabolism.

Furthermore, the KEGG enrichment analysis revealed that the lipid-related genes were primarily associated with the *PPAR* signaling pathway. *PPAR* is activated by fatty acids and their derivatives, thereby creating a lipid signaling network between the cell surface and the nucleus [40]. As lipid sensors and master regulators, *PPAR* controls the expression of genes that function in lipid metabolism [41]. The *PPAR* signaling pathway, a crossing regulator of lipid signaling and inflammation, [40] was enriched, indicating that it plays a crucial role in lipid metabolism response to AMI. A previous study has found that the downregulation of *PPAR* γ contributes to the activation and aggregation, eventually forming micro-thromboses, finally leading to myocardial dysfunction [42]. These results indicated that these lipid-related genes might affect AMI occurrence through the *PPAR* signaling pathway. However, further research is required to confirm the correlations between these key genes.

However, our current study also has some limitations. First, we used the dataset from circulating endothelial cells to perform the bioinformatics analysis, and used

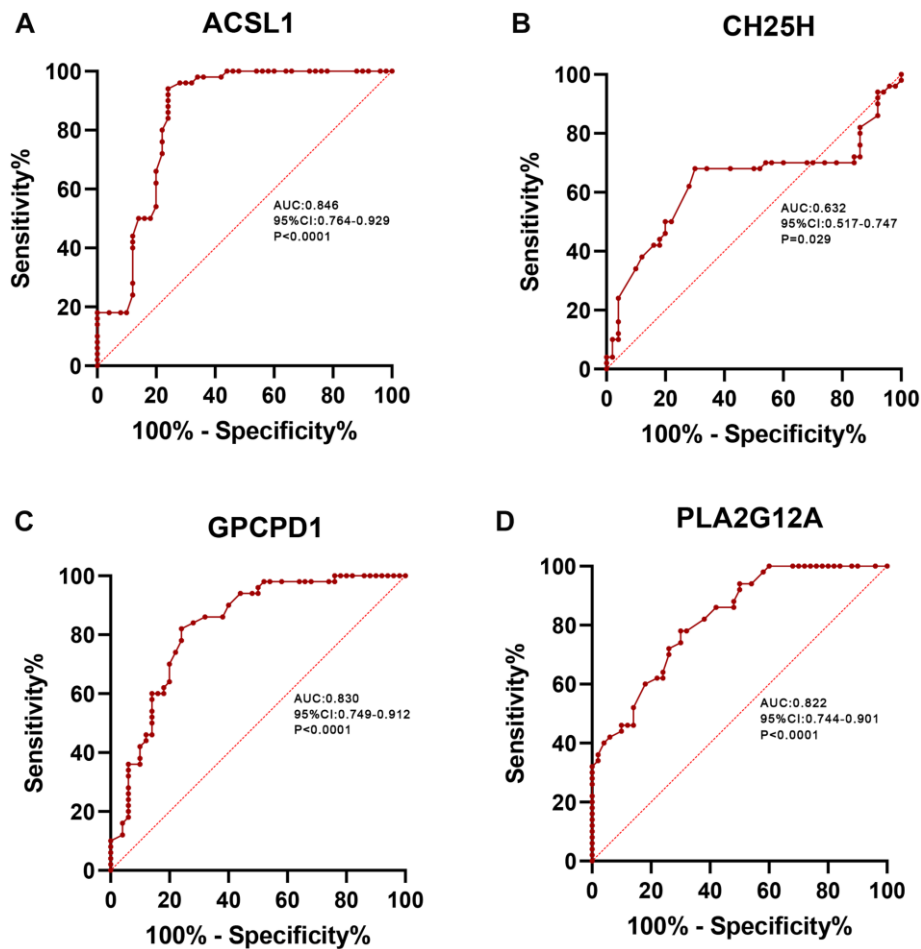


Figure 9. ROC curve analysis. ROC curve of *ACSL1* (A), *CH25H* (B), *GPCPD1* (C), *PLA2G12A* (D) in clinical samples.

the peripheral blood mononuclear cells from myocardial infarction and normal people for verification. Although there was some sample heterogeneity, our research, like other studies using GSE66360 dataset [43–45], obtained a satisfactory result, which fully supported our conclusion. However, more studies are needed to further confirm our findings. Second, the included clinical samples were relatively small. Therefore, our conclusions must be verified by a larger AMI cohort. Third, lipid-related DEGs were only confirmed in clinical samples, and their potential functions were not demonstrated in AMI cells or animal models. Hence, more *in vivo* and *in vitro* studies are needed to clarify the underlying mechanisms of these key genes in AMI.

In summary, four lipid-related genes involved in AMI were confirmed by bioinformatics analysis and machine learning methods. These genes might influence AMI occurrence by regulating lipid metabolism. Our current findings might help understand the mechanisms of lipid metabolism-related genes in AMI and develop future lipid-lowering treatment strategies for AMI.

MATERIALS AND METHODS

Lipid-related gene dataset

The workflow diagram of this research was shown in Supplementary Figure 1. A total of 742 lipid-related genes were retrieved from Gene Set Enrichment Analysis (<https://www.gsea-msigdb.org/gsea/index.jsp>) (Supplementary Table 3). The AMI dataset (GSE66360) was downloaded from the GEO website (<https://www.ncbi.nlm.nih.gov/geo/>). The GSE66360 dataset including a total of 99 circulating endothelial cell samples that collected from 49 AMI and 50 control subjects, and this dataset was based on the GPL570 platform (Affymetrix Human Genome U133 Plus 2.0 Array). A total of 21629 genes were detected in the GSE66360 dataset.

Identification of lipid-related DEGs

The “limma” R package was used to identify lipid-related DEGs between AMI patients and normal participants. The threshold values were $p < 0.05$ and $|\log \text{fold change (FC)}| > 0.585$ [46–48]. Heatmaps, volcano plots, and boxplot charts were plotted using “heatmap” and “ggplot2” R packages.

Functional enrichment analysis of lipid-related genes

The GO and KEGG pathway enrichment analyses were conducted using the “enrichplot” R package. Cell composition, biological processes, and molecular functions were included in the GO analysis.

Screening of lipid-related genes through SVM-RFE and LASSO logistic regression

The “glmnet” R package was used to perform LASSO logistic regression which the response type set as binomial and alpha set as 1 to identify lipid-related genes [49]. LASSO regression is a regularized penalty regression method, combining ridge regression and subset selection. It applies ordinary least squares, but the sum of absolute values of the regression coefficients is less than the predetermined constant value [50]. LASSO logistic regression is a generalization of the binomial distribution of the LASSO output variable. Herein, we used LASSO to screen lipid-related genes. Moreover, SVM-RFE is a machine learning method based on support vector machines that identify optimal variables by removing SVM-generated feature vectors [51], and the thresholds were set as follows: $\text{halve.above} = 100$ and $k = 5$. The “E1071” R package was used to establish the SVM module to sift lipid-related genes. Then, the intersections of lipid-related genes sifted by LASSO and SVM-RFE were applied to AMI diagnostic analysis, and the ROC curves were plotted.

Clinical validation samples

From September 2021 to May 2022, 50 AMI patients (AMI group) and healthy participants (control group) were recruited from the Hunan Provincial People’s Hospital. The blood samples were collected from AMI patients within hours of admission with chest pain and before using antiplatelet or anticoagulant to eliminate the influence of possible changes in blood status after pharmacological intervention. All AMI patients underwent percutaneous coronary intervention (PCI) within 12 h of the chest pain onset. The AMI patients were diagnosed based on the 2018 guidelines for diagnosing AMI patients [52]. A total of 50 healthy individuals were enrolled in the hospital physical examination center in the same period. The exclusion criteria were: (i) active inflammation; (ii) patients receiving thrombolysis and with other underlying heart diseases (e.g., severe valvular abnormalities, cardiomyopathy, or congenital heart disease); and (iii) patients who had hepatic and/or renal dysfunction, tumors, and autoimmune diseases. All participants provided written informed consent before the beginning of the study. This research was approved by the Ethics Committee of the Hunan Provincial People’s Hospital (approval number: [2021]-41).

Real-time quantitative polymerase chain reaction (RT-qPCR)

Peripheral blood was obtained from blood samples of patients using RNeasy™ Mini Kit (QIAGEN, Frankfurt,

Germany) to extract total RNA. Total RNA was reverse transcribed into cDNA using the PrimeScript RT reagent kit (Takara Bio, Japan). RT-qPCR was performed with a LightCycler 480 II Real-time PCR instrument (Roche, Switzerland) using the TransStart Top Green qPCR SuperMix (AQ131-03, Transgen, Beijing, China).

Statistical analysis

All bioinformatics and Pearson's correlation analyses were performed using R software (version 4.6.0, <http://www.R-project.org>). SPSS software (version 22.0) was used to analyze clinical data. Clinical characteristic data were analyzed using Student's *t*-test and χ^2 test. R and Graph Pad Prism software were used for ROC curve analysis. A $p < 0.05$ was considered statistically significant.

Abbreviations

AMI: acute myocardial infarction; DEGs: differentially expressed genes; GEO: Gene Expression Omnibus; GO: gene ontology; KEGG: Kyoto Encyclopedia of Genes and Genomes; LASSO: Least Absolute Shrinkage and Selector Operation; SVM-RFE: support vector machine recursive feature elimination; ROC: receiver operating characteristic; RT-qPCR: real-time quantitative polymerase chain reaction; LDL: low-density lipoprotein; VLDL: very low-density lipoprotein; MACEs: major adverse cardiovascular events; ACSL1: Acyl-CoA Synthetase Long-Chain Family Member 1; PLBD1: Phospholipase B Domain Containing 1; CH25H: Cholesterol 25-Hydroxylase; ELOVL4: ELOVL Fatty Acid Elongase 4; TNFAIP8L2: TNF Alpha Induced Protein 8 Like 2; CYP2E1: Cytochrome P450 Family 2 Subfamily E Member 1; GPCPD1: Glycerophosphocholine Phosphodiesterase 1; PLA2G12A: Phospholipase A2 Group XIIIA; AUC: area under the curve; CI: confidence interval; BMI: Body mass index; HDL-C: high-density lipoprotein cholesterol; LDL-C: low-density lipoprotein cholesterol; Apo: apolipoprotein; TC: total cholesterol; TG: triglyceride; CK: creatine kinase; CK-MB: creatine kinase-myocardial band.

AUTHOR CONTRIBUTIONS

Z.Y.L and F.L. designed the study, performed the statistical analyses and drafted the manuscript. P.F.Z and X.Q.H participated in the design and helped to draft the manuscript. F.L. collected the research data. H.W.P. performed the statistical analyses. S.L.P and Y.C. revised the manuscript. All authors read and approved the final manuscript.

ACKNOWLEDGMENTS

We thank all the participants of this study.

CONFLICTS OF INTEREST

The authors declare no conflicts of interest related to this study.

ETHICAL STATEMENT AND CONSENT

This research was approved by the Ethics Committee of the Hunan Provincial People's Hospital (approval number: [2021]-41.) Written informed consent was obtained from all participants.

FUNDING

This study was supported by the Key Research and Development Program of Hunan Province (No: 2019SK2021), Young Doctor Fund Project of Hunan Provincial People's Hospital (No: BSJJ202212) and the Natural Science Foundation of Hunan Province (No: 2020JJ4406). There was no role of the funding body in the design of the study and collection, analysis, and interpretation of data and in writing the manuscript.

REFERENCES

1. Yamada Y, Matsui K, Takeuchi I, Fujimaki T. Association of genetic variants with coronary artery disease and ischemic stroke in a longitudinal population-based genetic epidemiological study. *Biomed Rep.* 2015; 3:413–9. <https://doi.org/10.3892/br.2015.440> PMID:26137247
2. Abram S, Arruda-Olson AM, Scott CG, Pellikka PA, Nkomo VT, Oh JK, Milan A, Abidjan MM, McCully RB. Frequency, Predictors, and Implications of Abnormal Blood Pressure Responses During Dobutamine Stress Echocardiography. *Circ Cardiovasc Imaging.* 2017; 10:e005444. <https://doi.org/10.1161/CIRCIMAGING.116.005444> PMID:28351907
3. Chiu MH, Heydari B, Batulan Z, Maarouf N, Subramanya V, Schenck-Gustafsson K, O'Brien ER. Coronary artery disease in post-menopausal women: are there appropriate means of assessment? *Clin Sci (Lond).* 2018; 132:1937–52. <https://doi.org/10.1042/CS20180067> PMID:30185615
4. Madhavan MV, Gersh BJ, Alexander KP, Granger CB, Stone GW. Coronary Artery Disease in Patients ≥ 80 Years of Age. *J Am Coll Cardiol.* 2018; 71:2015–40.

- <https://doi.org/10.1016/j.jacc.2017.12.068>
PMID:[29724356](https://pubmed.ncbi.nlm.nih.gov/29724356/)
5. Anderson JL, Morrow DA. Acute Myocardial Infarction. *N Engl J Med.* 2017; 376:2053–64.
<https://doi.org/10.1056/NEJMra1606915>
PMID:[28538121](https://pubmed.ncbi.nlm.nih.gov/28538121/)
6. Andreadou I, Tsoumani M, Vilahur G, Ikonomidis I, Badimon L, Varga ZV, Ferdinandy P, Schulz R. PCSK9 in Myocardial Infarction and Cardioprotection: Importance of Lipid Metabolism and Inflammation. *Front Physiol.* 2020; 11:602497.
<https://doi.org/10.3389/fphys.2020.602497>
PMID:[33262707](https://pubmed.ncbi.nlm.nih.gov/33262707/)
7. Michos ED, McEvoy JW, Blumenthal RS. Lipid Management for the Prevention of Atherosclerotic Cardiovascular Disease. *N Engl J Med.* 2019; 381:1557–67.
<https://doi.org/10.1056/NEJMra1806939>
PMID:[31618541](https://pubmed.ncbi.nlm.nih.gov/31618541/)
8. Grundy SM, Cleeman JI, Merz CN, Brewer HB Jr, Clark LT, Hunninghake DB, Pasternak RC, Smith SC Jr, Stone NJ, and Coordinating Committee of the National Cholesterol Education Program. Implications of recent clinical trials for the National Cholesterol Education Program Adult Treatment Panel III Guidelines. *J Am Coll Cardiol.* 2004; 44:720–32.
<https://doi.org/10.1016/j.jacc.2004.07.001>
PMID:[15358046](https://pubmed.ncbi.nlm.nih.gov/15358046/)
9. Gotto AM Jr, Brinton EA. Assessing low levels of high-density lipoprotein cholesterol as a risk factor in coronary heart disease: a working group report and update. *J Am Coll Cardiol.* 2004; 43:717–24.
<https://doi.org/10.1016/j.jacc.2003.08.061>
PMID:[14998606](https://pubmed.ncbi.nlm.nih.gov/14998606/)
10. Gencer B, Koskinas KC, Räber L, Karagiannis A, Nanchen D, Auer R, Carballo D, Carballo S, Klingenberg R, Heg D, Matter CM, Lüscher TF, Rodondi N, et al. Eligibility for PCSK9 Inhibitors According to American College of Cardiology (ACC) and European Society of Cardiology/European Atherosclerosis Society (ESC/EAS) Guidelines After Acute Coronary Syndromes. *J Am Heart Assoc.* 2017; 6:e006537.
<https://doi.org/10.1161/JAHA.117.006537>
PMID:[29122809](https://pubmed.ncbi.nlm.nih.gov/29122809/)
11. Sinnaeve PR, Donahue MP, Grass P, Seo D, Vonderscher J, Chibout SD, Kraus WE, Sketch M Jr, Nelson C, Ginsburg GS, Goldschmidt-Clermont PJ, Granger CB. Gene expression patterns in peripheral blood correlate with the extent of coronary artery disease. *PLoS One.* 2009; 4:e7037.
<https://doi.org/10.1371/journal.pone.0007037>
PMID:[19750006](https://pubmed.ncbi.nlm.nih.gov/19750006/)
12. Muse ED, Kramer ER, Wang H, Barrett P, Parviz F, Novotny MA, Lasken RS, Jatko TA, Oliveira G, Peng H, Lu J, Connelly MC, Schilling K, et al. A Whole Blood Molecular Signature for Acute Myocardial Infarction. *Sci Rep.* 2017; 7:12268.
<https://doi.org/10.1038/s41598-017-12166-0>
PMID:[28947747](https://pubmed.ncbi.nlm.nih.gov/28947747/)
13. Ntzani EE, Ioannidis JP. Predictive ability of DNA microarrays for cancer outcomes and correlates: an empirical assessment. *Lancet.* 2003; 362:1439–44.
[https://doi.org/10.1016/S0140-6736\(03\)14686-7](https://doi.org/10.1016/S0140-6736(03)14686-7)
PMID:[14602436](https://pubmed.ncbi.nlm.nih.gov/14602436/)
14. Ein-Dor L, Kela I, Getz G, Givol D, Domany E. Outcome signature genes in breast cancer: is there a unique set? *Bioinformatics.* 2005; 21:171–8.
<https://doi.org/10.1093/bioinformatics/bth469>
PMID:[15308542](https://pubmed.ncbi.nlm.nih.gov/15308542/)
15. Chen R, Liu X, Jin S, Lin J, Liu J. Machine Learning for Drug-Target Interaction Prediction. *Molecules.* 2018; 23:30200333.
<https://doi.org/10.3390/molecules23092208>
PMID:[30200333](https://pubmed.ncbi.nlm.nih.gov/30200333/)
16. Wei S, Lu J, Lou J, Shi C, Mo S, Shao Y, Ni J, Zhang W, Cheng X. Gastric Cancer Tumor Microenvironment Characterization Reveals Stromal-Related Gene Signatures Associated With Macrophage Infiltration. *Front Genet.* 2020; 11:663.
<https://doi.org/10.3389/fgene.2020.00663>
PMID:[32695142](https://pubmed.ncbi.nlm.nih.gov/32695142/)
17. Kumar R, Indrayan A. Receiver operating characteristic (ROC) curve for medical researchers. *Indian Pediatr.* 2011; 48:277–87.
<https://doi.org/10.1007/s13312-011-0055-4>
PMID:[21532099](https://pubmed.ncbi.nlm.nih.gov/21532099/)
18. Moreira DM, da Silva RL, Vieira JL, Fattah T, Lueneberg ME, Gottschall CA. Role of vascular inflammation in coronary artery disease: potential of anti-inflammatory drugs in the prevention of atherothrombosis. Inflammation and anti-inflammatory drugs in coronary artery disease. *Am J Cardiovasc Drugs.* 2015; 15:1–11.
<https://doi.org/10.1007/s40256-014-0094-z>
PMID:[25369900](https://pubmed.ncbi.nlm.nih.gov/25369900/)
19. Boateng S, Sanborn T. Acute myocardial infarction. *Dis Mon.* 2013; 59:83–96.
<https://doi.org/10.1016/j.disamonth.2012.12.004>
PMID:[23410669](https://pubmed.ncbi.nlm.nih.gov/23410669/)
20. Ferrières J, Amber V, Crisan O, Chazelle F, Jünger C, Wood D. Total lipid management and cardiovascular disease in the dyslipidemia international study. *Cardiology.* 2013; 125:154–63.
<https://doi.org/10.1159/000348859>
PMID:[23736147](https://pubmed.ncbi.nlm.nih.gov/23736147/)

21. Chapman MJ, Ginsberg HN, Amarenco P, Andreotti F, Borén J, Catapano AL, Descamps OS, Fisher E, Kovanen PT, Kuivenhoven JA, Lesnik P, Masana L, Nordestgaard BG, et al, and European Atherosclerosis Society Consensus Panel. Triglyceride-rich lipoproteins and high-density lipoprotein cholesterol in patients at high risk of cardiovascular disease: evidence and guidance for management. *Eur Heart J*. 2011; 32:1345–61.
<https://doi.org/10.1093/eurheartj/ehr112>
PMID:[21531743](https://pubmed.ncbi.nlm.nih.gov/21531743/)
22. Can M, Acikgoz S, Mungan G, Ugurbas E, Ankarali H, Sumbuloglu V, Demirtas S, Karaca L. Is direct method of low density lipoprotein cholesterol measurement appropriate for targeting lipid lowering therapy? *Int J Cardiol*. 2010; 142:105–7.
<https://doi.org/10.1016/j.ijcard.2008.11.141>
PMID:[19135270](https://pubmed.ncbi.nlm.nih.gov/19135270/)
23. Zdravkovic S, Wienke A, Pedersen NL, de Faire U. Genetic susceptibility of myocardial infarction. *Twin Res Hum Genet*. 2007; 10:848–52.
<https://doi.org/10.1375/twin.10.6.848>
PMID:[18179397](https://pubmed.ncbi.nlm.nih.gov/18179397/)
24. Zhao YP, Wang JJ, Li XY, Peng GJ, Yang Z. Extended least squares support vector machine with applications to fault diagnosis of aircraft engine. *ISA Trans*. 2020; 97:189–201.
<https://doi.org/10.1016/j.isatra.2019.08.036>
PMID:[31488246](https://pubmed.ncbi.nlm.nih.gov/31488246/)
25. Wan JJ, Chen BL, Kong YX, Ma XG, Yu YT. An Early Intestinal Cancer Prediction Algorithm Based on Deep Belief Network. *Sci Rep*. 2019; 9:17418.
<https://doi.org/10.1038/s41598-019-54031-2>
PMID:[31758076](https://pubmed.ncbi.nlm.nih.gov/31758076/)
26. Goldenberg JR, Wang X, Lewandowski ED. Acyl CoA synthetase-1 links facilitated long chain fatty acid uptake to intracellular metabolic trafficking differently in hearts of male versus female mice. *J Mol Cell Cardiol*. 2016; 94:1–9.
<https://doi.org/10.1016/j.yjmcc.2016.03.006>
PMID:[26995156](https://pubmed.ncbi.nlm.nih.gov/26995156/)
27. Li LO, Ellis JM, Paich HA, Wang S, Gong N, Altshuler G, Thresher RJ, Koves TR, Watkins SM, Muoio DM, Cline GW, Shulman GI, Coleman RA. Liver-specific loss of long chain acyl-CoA synthetase-1 decreases triacylglycerol synthesis and beta-oxidation and alters phospholipid fatty acid composition. *J Biol Chem*. 2009; 284:27816–26.
<https://doi.org/10.1074/jbc.M109.022467>
PMID:[19648649](https://pubmed.ncbi.nlm.nih.gov/19648649/)
28. Chiu HC, Kovacs A, Ford DA, Hsu FF, Garcia R, Herrero P, Saffitz JE, Schaffer JE. A novel mouse model of lipotoxic cardiomyopathy. *J Clin Invest*. 2001; 107:813–22.
<https://doi.org/10.1172/JCI10947>
PMID:[11285300](https://pubmed.ncbi.nlm.nih.gov/11285300/)
29. Li Y, Yang M, Tan J, Shen C, Deng S, Fu X, Gao S, Li H, Zhang X, Cai W. Targeting ACSL1 promotes cardiomyocyte proliferation and cardiac regeneration. *Life Sci*. 2022; 294:120371.
<https://doi.org/10.1016/j.lfs.2022.120371>
PMID:[35122795](https://pubmed.ncbi.nlm.nih.gov/35122795/)
30. Yang L, Yang Y, Si D, Shi K, Liu D, Meng H, Meng F. High expression of long chain acyl-coenzyme A synthetase 1 in peripheral blood may be a molecular marker for assessing the risk of acute myocardial infarction. *Exp Ther Med*. 2017; 14:4065–72.
<https://doi.org/10.3892/etm.2017.5091>
PMID:[29104625](https://pubmed.ncbi.nlm.nih.gov/29104625/)
31. Li T, Li X, Meng H, Chen L, Meng F. ACSL1 affects Triglyceride Levels through the PPARγ Pathway. *Int J Med Sci*. 2020; 17:720–7.
<https://doi.org/10.7150/ijms.42248>
PMID:[32218693](https://pubmed.ncbi.nlm.nih.gov/32218693/)
32. Wang VM, Rosen RB, Meyerle CB, Kurup SK, Ardeljan D, Agron E, Tai K, Pomykala M, Chew EY, Chan CC, Tuo J. Suggestive association between PLA2G12A single nucleotide polymorphism rs2285714 and response to anti-vascular endothelial growth factor therapy in patients with exudative age-related macular degeneration. *Mol Vis*. 2012; 18:2578–85.
PMID:[23112570](https://pubmed.ncbi.nlm.nih.gov/23112570/)
33. Nicolaou A, Northoff BH, Sass K, Ernst J, Kohlmaier A, Krohn K, Wolfrum C, Teupser D, Holdt LM. Quantitative trait locus mapping in mice identifies phospholipase Pla2g12a as novel atherosclerosis modifier. *Atherosclerosis*. 2017; 265:197–206.
<https://doi.org/10.1016/j.atherosclerosis.2017.08.030>
PMID:[28917158](https://pubmed.ncbi.nlm.nih.gov/28917158/)
34. Tuong ZK, Lau P, Du X, Condon ND, Goode JM, Oh TG, Yeo JC, Muscat GE, Stow JL. RORα and 25-Hydroxycholesterol Crosstalk Regulates Lipid Droplet Homeostasis in Macrophages. *PLoS One*. 2016; 11:e0147179.
<https://doi.org/10.1371/journal.pone.0147179>
PMID:[26812621](https://pubmed.ncbi.nlm.nih.gov/26812621/)
35. Zhao J, Chen J, Li M, Chen M, Sun C. Multifaceted Functions of CH25H and 25HC to Modulate the Lipid Metabolism, Immune Responses, and Broadly Antiviral Activities. *Viruses*. 2020; 12:727.
<https://doi.org/10.3390/v12070727>
PMID:[32640529](https://pubmed.ncbi.nlm.nih.gov/32640529/)
36. Gold ES, Ramsey SA, Sartain MJ, Selinummi J, Podolsky I, Rodriguez DJ, Moritz RL, Aderem A. ATF3 protects against atherosclerosis by suppressing 25-hydroxycholesterol-induced lipid body formation. *J Exp Med*. 2012; 209:807–17.

- <https://doi.org/10.1084/jem.20111202>
PMID:22473958
37. Li Z, Martin M, Zhang J, Huang HY, Bai L, Zhang J, Kang J, He M, Li J, Maurya MR, Gupta S, Zhou G, Sangwung P, et al. Krüppel-Like Factor 4 Regulation of Cholesterol-25-Hydroxylase and Liver X Receptor Mitigates Atherosclerosis Susceptibility. *Circulation*. 2017; 136:1315–30.
<https://doi.org/10.1161/CIRCULATIONAHA.117.027462>
PMID:28794002
38. Marchan R, Büttner B, Lambert J, Edlund K, Glaeser I, Blaszkewicz M, Leonhardt G, Marienhoff L, Kaszta D, Anft M, Watzl C, Madjar K, Grinberg M, et al. Glycerol-3-phosphate Acyltransferase 1 Promotes Tumor Cell Migration and Poor Survival in Ovarian Carcinoma. *Cancer Res*. 2017; 77:4589–601.
<https://doi.org/10.1158/0008-5472.CAN-16-2065>
PMID:28652252
39. Glunde K, Penet MF, Jiang L, Jacobs MA, Bhujwala ZM. Choline metabolism-based molecular diagnosis of cancer: an update. *Expert Rev Mol Diagn*. 2015; 15:735–47.
<https://doi.org/10.1586/14737159.2015.1039515>
PMID:25921026
40. Wahli W, Michalik L. PPARs at the crossroads of lipid signaling and inflammation. *Trends Endocrinol Metab*. 2012; 23:351–63.
<https://doi.org/10.1016/j.tem.2012.05.001>
PMID:22704720
41. Michalik L, Auwerx J, Berger JP, Chatterjee VK, Glass CK, Gonzalez FJ, Grimaldi PA, Kadowaki T, Lazar MA, O'Rahilly S, Palmer CN, Plutzky J, Reddy JK, et al. International Union of Pharmacology. LXI. Peroxisome proliferator-activated receptors. *Pharmacol Rev*. 2006; 58:726–41.
<https://doi.org/10.1124/pr.58.4.5>
PMID:17132851
42. Zhou H, Li D, Zhu P, Hu S, Hu N, Ma S, Zhang Y, Han T, Ren J, Cao F, Chen Y. Melatonin suppresses platelet activation and function against cardiac ischemia/reperfusion injury via PPAR γ /FUNDC1/mitophagy pathways. *J Pineal Res*. 2017; 63:e12438.
<https://doi.org/10.1111/jpi.12438>
PMID:28749565
43. Zheng PF, Liao FJ, Yin RX, Chen LZ, Li H, Nie RJ, Wang Y, Liao PJ. Genes associated with inflammation may serve as biomarkers for the diagnosis of coronary artery disease and ischaemic stroke. *Lipids Health Dis*. 2020; 19:37.
<https://doi.org/10.1186/s12944-020-01217-7>
PMID:32164735
44. Cheng M, An S, Li J. Identifying key genes associated with acute myocardial infarction. *Medicine (Baltimore)*. 2017; 96:e7741.
<https://doi.org/10.1097/MD.0000000000007741>
PMID:29049183
45. Ji Z, Zhang R, Yang M, Zuo W, Yao Y, Qu Y, Su Y, Liu Z, Gu Z, Ma G. Accuracy of triggering receptor expressed on myeloid cells 1 in diagnosis and prognosis of acute myocardial infarction: a prospective cohort study. *PeerJ*. 2021; 9:e11655.
<https://doi.org/10.7717/peerj.11655>
PMID:34221733
46. Xia C, Chen L, Sun W, Yan R, Xia M, Wang Y, Yang D. Total saponins from *Paris forrestii* (Takht) H. Li. show the anticancer and RNA expression regulating effects on prostate cancer cells. *Biomed Pharmacother*. 2020; 121:109674.
<https://doi.org/10.1016/j.biopha.2019.109674>
PMID:31810132
47. Huang J, Liu L, Qin L, Huang H, Li X. Weighted Gene Coexpression Network Analysis Uncovers Critical Genes and Pathways for Multiple Brain Regions in Parkinson's Disease. *Biomed Res Int*. 2021; 2021:6616434.
<https://doi.org/10.1155/2021/6616434>
PMID:33791366
48. Xu M, Li Z, Yang L, Zhai W, Wei N, Zhang Q, Chao B, Huang S, Cui H. Elucidation of the Mechanisms and Molecular Targets of *Sanhuang Xiexin* Decoction for Type 2 Diabetes Mellitus Based on Network Pharmacology. *Biomed Res Int*. 2020; 2020:5848497.
<https://doi.org/10.1155/2020/5848497>
PMID:32851081
49. McEligot AJ, Poynor V, Sharma R, Panangadan A. Logistic LASSO Regression for Dietary Intakes and Breast Cancer. *Nutrients*. 2020; 12:2652.
<https://doi.org/10.3390/nu12092652>
PMID:32878103
50. Pierre JF, Akbilgic O, Smallwood H, Cao X, Fitzpatrick EA, Pena S, Furmanek SP, Ramirez JA, Jonsson CB. Discovery and predictive modeling of urine microbiome, metabolite and cytokine biomarkers in hospitalized patients with community acquired pneumonia. *Sci Rep*. 2020; 10:13418.
<https://doi.org/10.1038/s41598-020-70461-9>
PMID:32770049
51. Sundermann B, Bode J, Lueken U, Westphal D, Gerlach AL, Straube B, Wittchen HU, Ströhle A, Wittmann A, Konrad C, Kircher T, Arolt V, Pfeleiderer B. Support Vector Machine Analysis of Functional Magnetic Resonance Imaging of Interoception Does Not Reliably Predict Individual Outcomes of Cognitive

Behavioral Therapy in Panic Disorder with Agoraphobia. *Front Psychiatry*. 2017; 8:99.

<https://doi.org/10.3389/fpsy.2017.00099>

PMID:[28649205](https://pubmed.ncbi.nlm.nih.gov/28649205/)

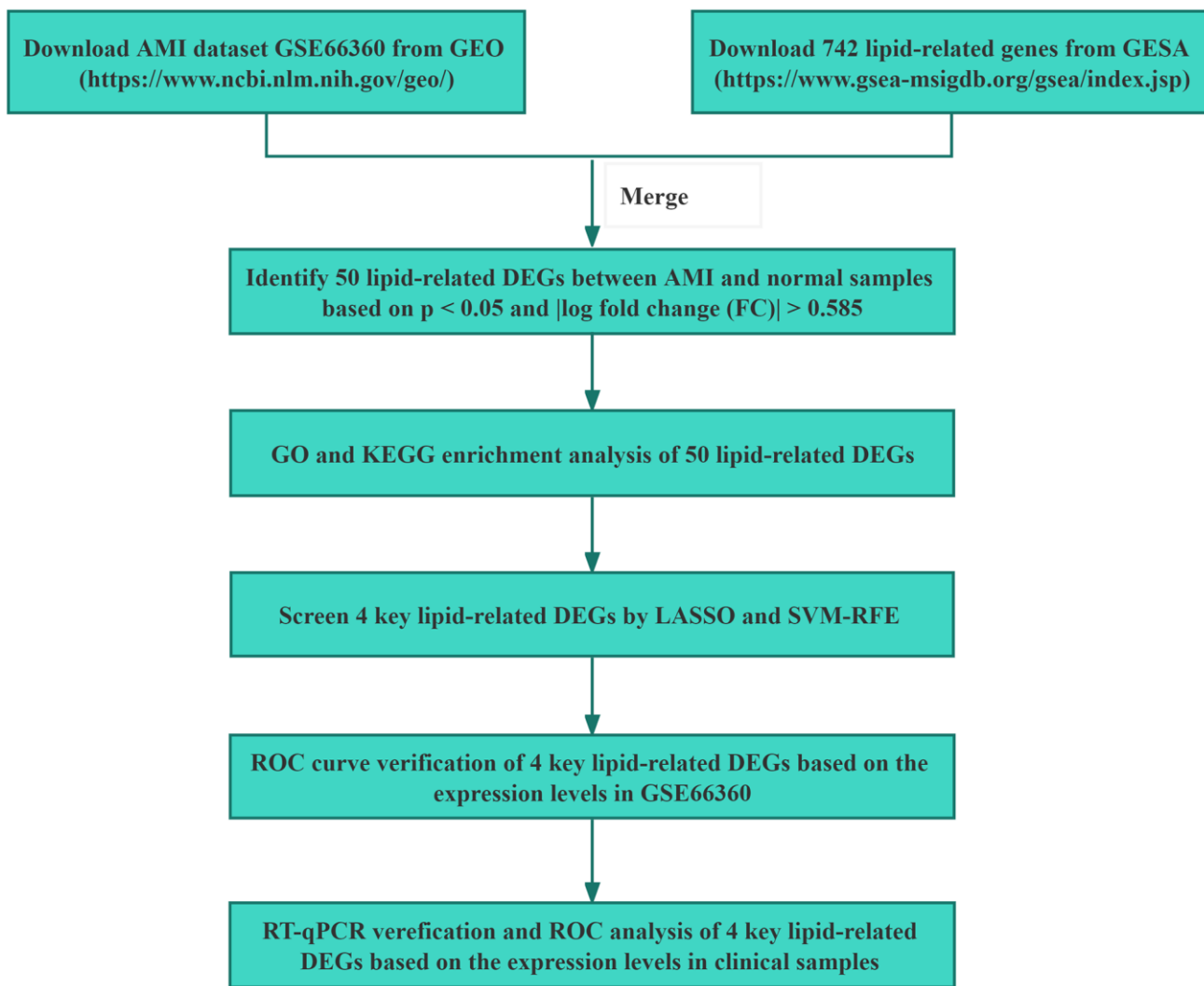
52. Thygesen K, Alpert JS, Jaffe AS, Chaitman BR, Bax JJ, Morrow DA, White HD, and Executive Group on behalf of the Joint European Society of Cardiology (ESC)/American College of Cardiology (ACC)/American Heart Association (AHA)/World Heart Federation (WHF) Task Force for the Universal Definition of Myocardial Infarction. Fourth Universal Definition of Myocardial Infarction (2018). *Circulation*. 2018; 138:e618–51.

<https://doi.org/10.1161/CIR.0000000000000617>

PMID:[30571511](https://pubmed.ncbi.nlm.nih.gov/30571511/)

SUPPLEMENTARY MATERIALS

Supplementary Figure



Supplementary Figure 1. A flow chart for analysis.

Supplementary Tables

Please browse Full Text version to see the data of Supplementary Tables 1 and 3.

Supplementary Table 1. Functional annotation of the DEGs.

Supplementary Table 2. Key genes identified by LASSO and SVM-RFE.

Names	Total	GENES
LASSO SVM-RFE	4	ACSL1 CH25H PLA2G12A GPCPD1
LASSO	15	ACSL1 CH25H HSD11B1 CYP1B1 BMX PLA2G12A GPCPD1 CROT ARV1 TBXAS1 GK3P LCLAT1 ALOX5AP ORMDL2 STARD4
SVM-RFE	4	GPCPD1 ACSL1 CH25H PLA2G12A

Supplementary Table 3. Summary of 742 lipid-related genes.